Integrated Pan-Arctic Melt Onset Detection from Satellite Microwave Measurements

LIBO WANG[1], CHRIS DERKSEN[1] , STEPHEN HOWELL[1] , GABRIEL J. WOLKEN[2], MARTIN SHARP[2] , AND THORSTEN MARKUS [3]

ABSTRACT

Due to its high sensitivity to the appearance of liquid water in snow and day/night all weather capability, satellite-borne microwave scatterometer and radiometer data have been successfully used to detect melt onset on various elements of the cryosphere. In this study, we combine active and passive microwave satellite derived melt onset estimates from unique, previously published, algorithms developed for the northern high latitude land surface, ice caps, large lakes, and sea ice. Comparisons of melt onset along the boundaries between different components of the cryosphere show that the integrated dataset can provide consistent melt onset in most areas of the pan-Arctic region, thereby characterizing the annual and inter-annual variability in melt timing across the pan-Arctic. This dataset provides a unique tool to study the relationship among different components of the cryosphere and to investigate the atmospheric conditions associated with different melt onset patterns in the Arctic.

Keywords: melt onset, sea ice, QuikSCAT, SSM/I, pan-Arctic

INTRODUCTION

Arctic sea ice extent and thickness has decreased considerably in the last decade (Comiso et al., 2008; Haas et al., 2008). Contrasting to the rapid reduction in Arctic sea ice, however, there is no linear decrease in Arctic spring snow cover duration over the past decade (Derksen et al., 2009). Satellite microwave data from the SeaWinds scatterometer on QuikSCAT (QS) and from the Special Sensor Microwave Imager (SSM/I) have been used to monitor the timing of spring snowmelt onset on various surfaces of the northern high latitude regions. Optimized algorithms have been developed to detect melt onset for the land surface (Wang et al., 2008), ice caps (Sharp and Wang, 2009), large lakes (Howell et al., 2009), and sea ice (Howell et al., 2008; Markus et al., submitted; Stroeve et al., 2006). The onset of snowmelt is important to determine because it greatly reduces the surface albedo and thus affects the surface energy balance. It is closely related to the stability of permafrost, the length of growing season, and sea ice extent during the summer.

In this study, we combine melt onset datasets derived from scatterometer and radiometer measurements for various elements of the cryosphere during the 2000 – 2008 period. We evaluate

[1]Climate Research Division, Atmospheric Science and Technology Directorate, Environment Canada, Toronto, Ontario, Canada.

[2]Department of Earth and Atmospheric Sciences, University of Alberta, Edmonton, Alberta, Canada.

[3]Cryospheric Sciences Branch, Code 614.1, NASA Goddard Space Flight Center, Greenbelt, MD.

the consistency of the integrated dataset and present the annual and inter-annual variability of melt onset across the pan-Arctic.

METHODOLOGY

A small amount of liquid water in snow causes a large dielectric contrast, which greatly reduces volume scattering and decreases radar backscatter (σ^0). This serves as the basis for melt detection from time series of enhanced resolution (~4.5km) QS scatterometer measurements (Fig.1).

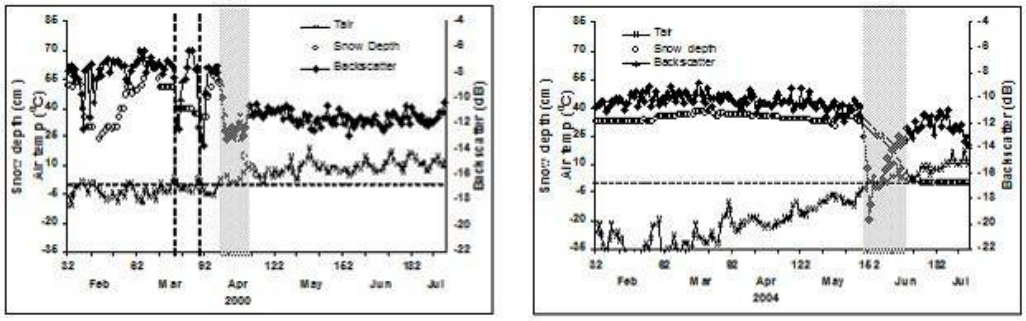

Figure 1. Time series of QS backscatter, air temperature and snow depth observations at a forest site (left) and a tundra site (right). The vertical dashed line represents the estimated onset date of preliminary melt events. The shaded grey bar represents the duration of the main melt event.

Threshold techniques have been applied to QS data to retrieve melt parameters for terrestrial snow cover, lake ice, ice caps, and Canadian Arctic Archipelago (CAA) sea ice. Melt detection algorithms for each surface type are summarized in the following:

Terrestrial snow: melt events were detected if the daily σ° was 1.7dB lower than the previous 5-day average for three or more consecutive days. The main melt event was identified as the event with the longest melt duration or the maximum melt intensity. The algorithm is capable of distinguishing preliminary melt events from the main melt event, and recognizes and excludes areas for which a snow melt event cannot be determined to prevent erroneous melt retrievals (Wang et al., 2008).

Ice caps/Greenland: based on previous melt detection methods (Sharp and Wang, 2009), an optimized single set of thresholds was developed to estimate melt onset for all the ice caps in the high Arctic and Greenland. Onset was determined when either: (i) change in σ° was 3.0 dB greater than the winter mean σ° for 3 or more consecutive days, or (ii) change in σ° was 3.5 dB greater than the winter mean for 1 day.

Lake ice: melt onset over Great Bear Lake and Great Slave Lake was determined when change in σ° was 4 dB greater than the winter mean σ° for 2 or more consecutive days (Howell et al., 2009).

CAA sea ice: melt onset was estimated using a threshold of absolute change in σ° of greater than 2dB from winter conditions. The algorithm was applied to homogenous FYI (< -18dB) and MYI (< -11 dB) pixels identified during the winter season. A kriging interpolation method was applied to estimate spatially continuous onset dates in the CAA (Howell et al., 2006).

Melt onset on sea ice outside the CAA was estimated from Special Sensor Microwave/Imager (SSM/I) passive microwave brightness temperatures (Tb). Based on previous methods (Drobot and Anderson, 2001; Belchansky et al., 2004; and Smith et al., 1998), multiple melt indicators were used to determine melt onset (Markus et al. submitted). The three primary indicators were: daily change in 37V, spectral gradient ratio for 37V and 19V, and a P parameter (P=Tb(19V)+0.8Tb(37V)). The strength of the melt signal was determined by summing up the normalized magnitude for each indicator. The day with the greatest sum was the melt onset day, the second peak was the early melt day. “Early melt” was defined as the transition period when the

snow pack starts transformation due to melt-freeze cycles; "melt onset" was defined as the day when free water is continuously present in the snow pack, after which the sea ice stays under melt conditions for the remainder of the summer.

The SSM/I-derived melt dataset also covers sea ice in CAA. Comparison of melt onset in the Queen Elisabeth Islands (QEI) region (Fig.2) shows that the QS-derived melt onset (yellow line) for CAA sea ice agrees better with the SSM/I-derive early melt (pink line). SSM/I-derived early melt also matches more closely with melt onset over adjacent land surfaces (Fig.5). Thus early melt from SSM/I for the Arctic basin and QS-derived melt onset elsewhere were used to produce the integrated melt onset in the pan-Arctic region during 2000-2008 (Fig.3). Standardized melt onset anomalies were calculated relative to the mean of the 2000-2008 period (Fig. 4).

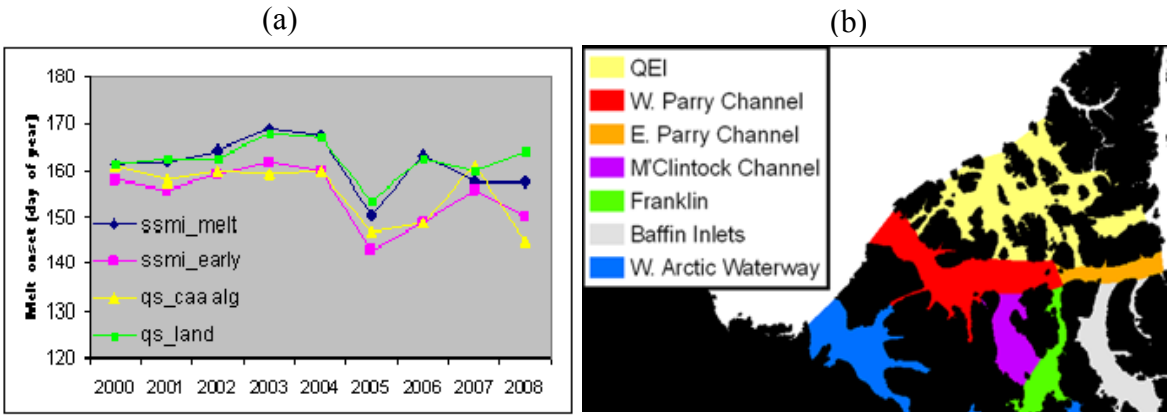

Figure 2. (a) Average melt onset dates for all pixels in the QEI sea ice region from QS and from SSM/I data; (b) sea ice regions in the Canadian Arctic Archipelago.

RESULTS AND DISCUSSION

Snowmelt onset is closely related to land cover and topography (Fig.3). On average, melt starts in the middle to the end of March for boreal forest at lower latitudes, with the date of melt onset becomes later with increasing latitude. For the Arctic tundra, melt does not typically start until late May to June. High relief areas were resolved well in the melt onset map with later melt onset over high elevation areas than the surrounding lowlands. In the Arctic basin, melt usually starts from mid-May in the Chukchi sea region, then spreads to the Beaufort sea and the East Siberia sea. Melt reaches the central Arctic by mid-June. Melt on the ice caps/Greenland occurs much later than the adjacent land/sea ice due to elevation differences. For the Arctic continental mainland, the average melt onset was latest in the central Siberia tundra region during the study period (Fig.3a). This was also true in each year during the 2000 to 2008 period except for 2000 and 2007, in which the latest melt onset occurred in the Canadian Arctic tundra (Fig.3b&3i). In general melt onset was later for the eastern Arctic sea ice than for the western Arctic sea ice.

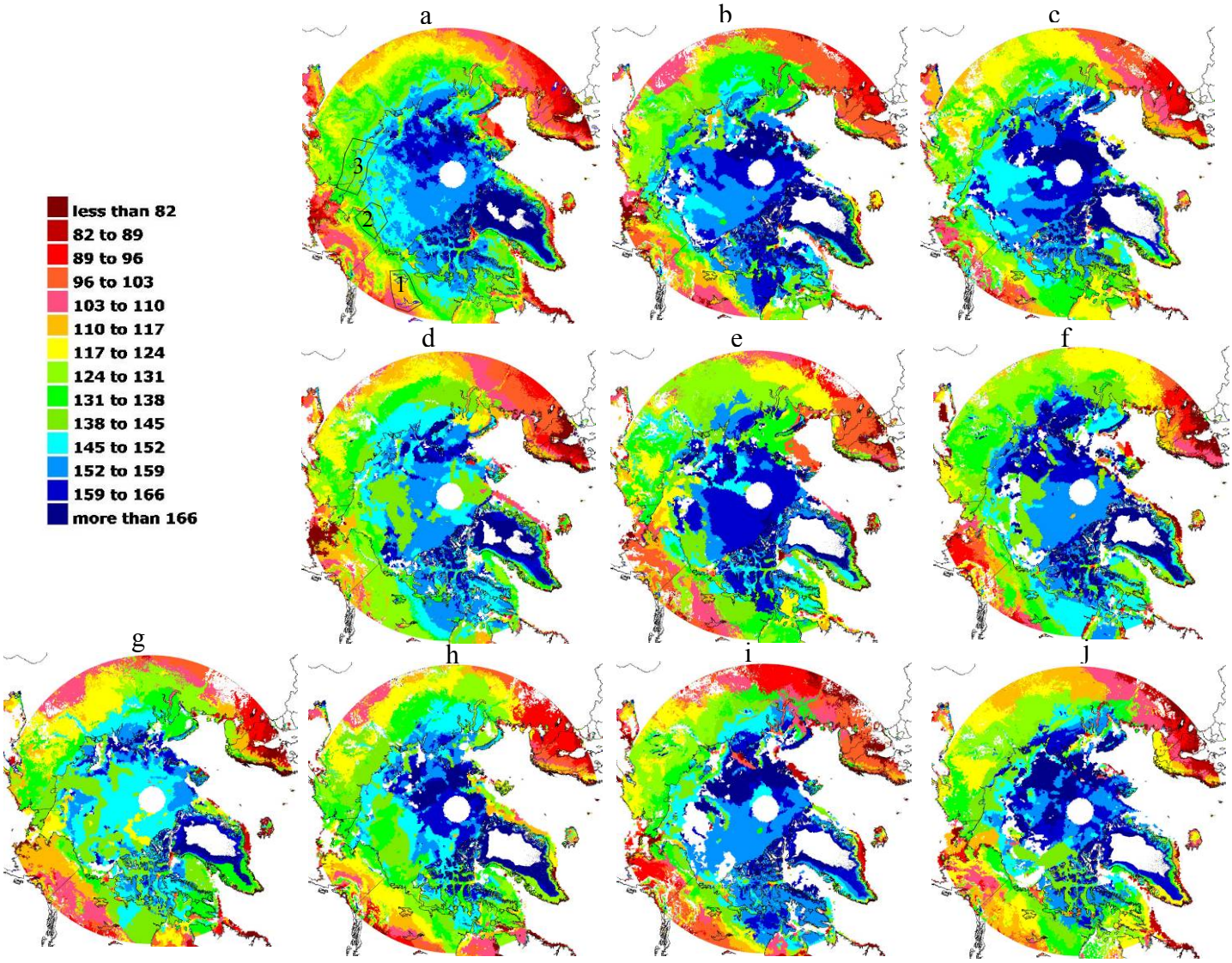

Figure 3. Integrated pan-Arctic melt onset during 2000 – 2008, (a) mean melt onset during 2000 – 2008; (b) 2000; (c) 2001; (d) 2002; (e) 2003; (f) 2004; (g) 2005; (h) 2006; (i) 2007; (j) 2008. White colour represents areas with melt not detected.

Snowmelt was not detected on some terrestrial, sea ice, and the high elevation areas of the Greenland ice sheet (white coloured area in Fig.3). These are however due to very different reasons. On terrestrial snow cover, melt may not be detected by QS data because melt signal can either be diminished by dense forest cover or be transient in thin snow cover regions (Wang at el. 2008). On the Arctic sea ice, melt may not be detected by the SSM/I data mostly in the marginal seas, which is mainly due to sea ice dynamics and ocean currents (Stroeve et al., 2006). On the Greenland ice sheet, melt does not always occur for areas above 2500m and melt seldom reaches the summit area (Wang et al., 2007).

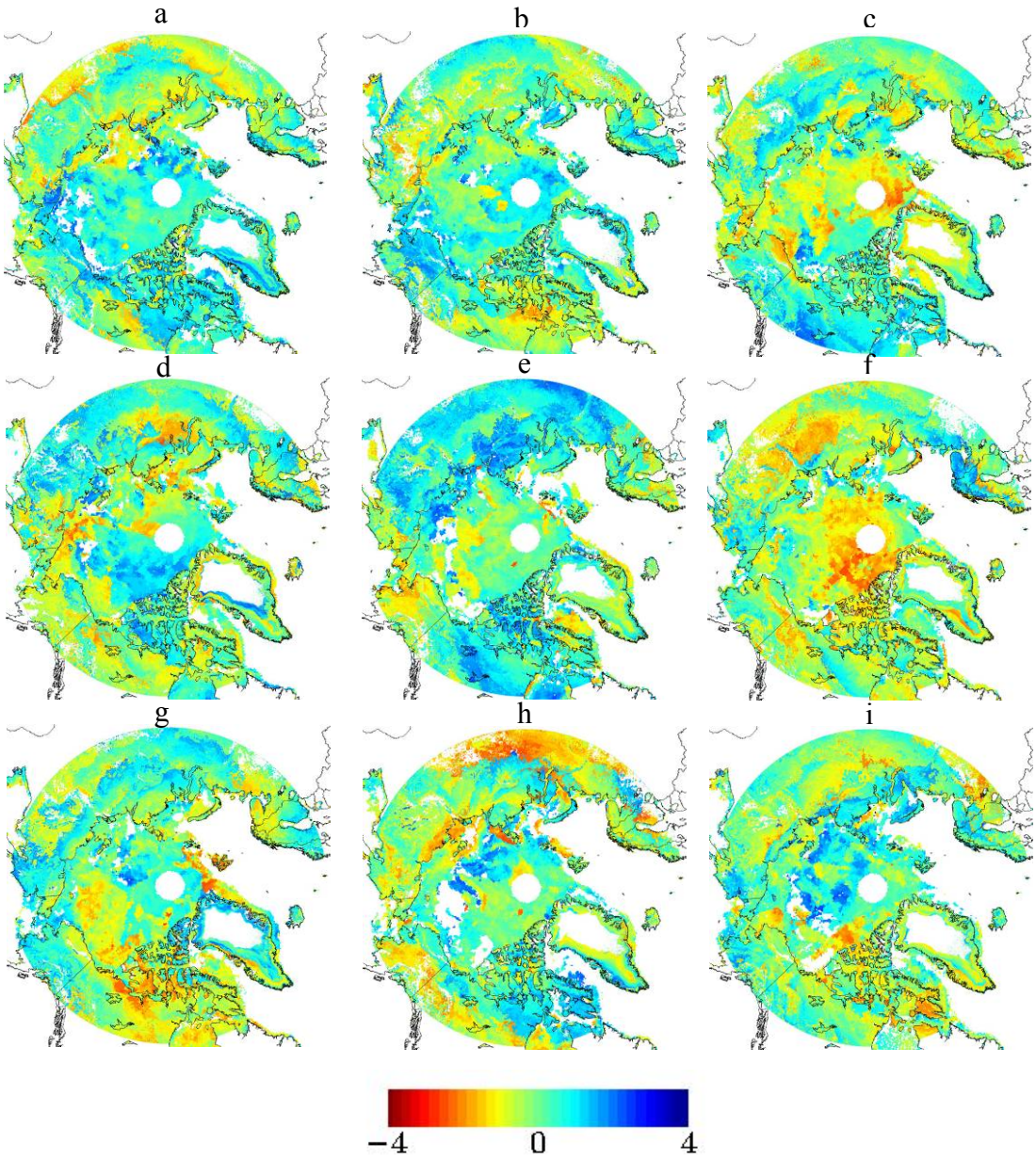

Figure 4. Standardized melt onset anomaly during 2000 – 2008, (a) 2000; (b) 2001; (c) 2002; (d) 2003; (e) 2004; (f) 2005; (g) 2006; (h) 2007; (i) 2008. White colour represents areas with melt not detected.

There are large annual and inter-annual variability in the anomalies of melt onset across the pan-Arctic (Fig.4). In 2002 and 2005, the onset of melt was anomalously early for the Arctic sea ice (Fig. 4c&4f). This has probably contributed to the previous record minimum sea ice extent in these two summers as the total amount of solar energy absorbed by the ice and ocean was strongly related to the date of melt onset (Perovich et al., 2007). Pre-conditioning, increased basal melt, and anomalously sunny skies likely played more of a role than early melt onset for 2007 and 2008 (Kay et al. 2008; Perovich et al. 2008; Stroeve et al. 2008). Melt onset was also anomalously early on most land areas in 2005, while it was mostly late on land in 2002. Onset of melt was anomalously late on most land areas in 2004. For the other years, there were no dominating signs in the anomalies of melt onset across the Arctic. It varies from region to region. On the ice caps in QEI, onset of melt occurred anomalously early in 2000, 2005 and 2008, it was anomalously late in

2002, 2004, and 2006. On the Greenland ice sheet, 2002 had the maximum melt extent and the earliest melt onset during the study period (Fig.3d and Fig.4c).

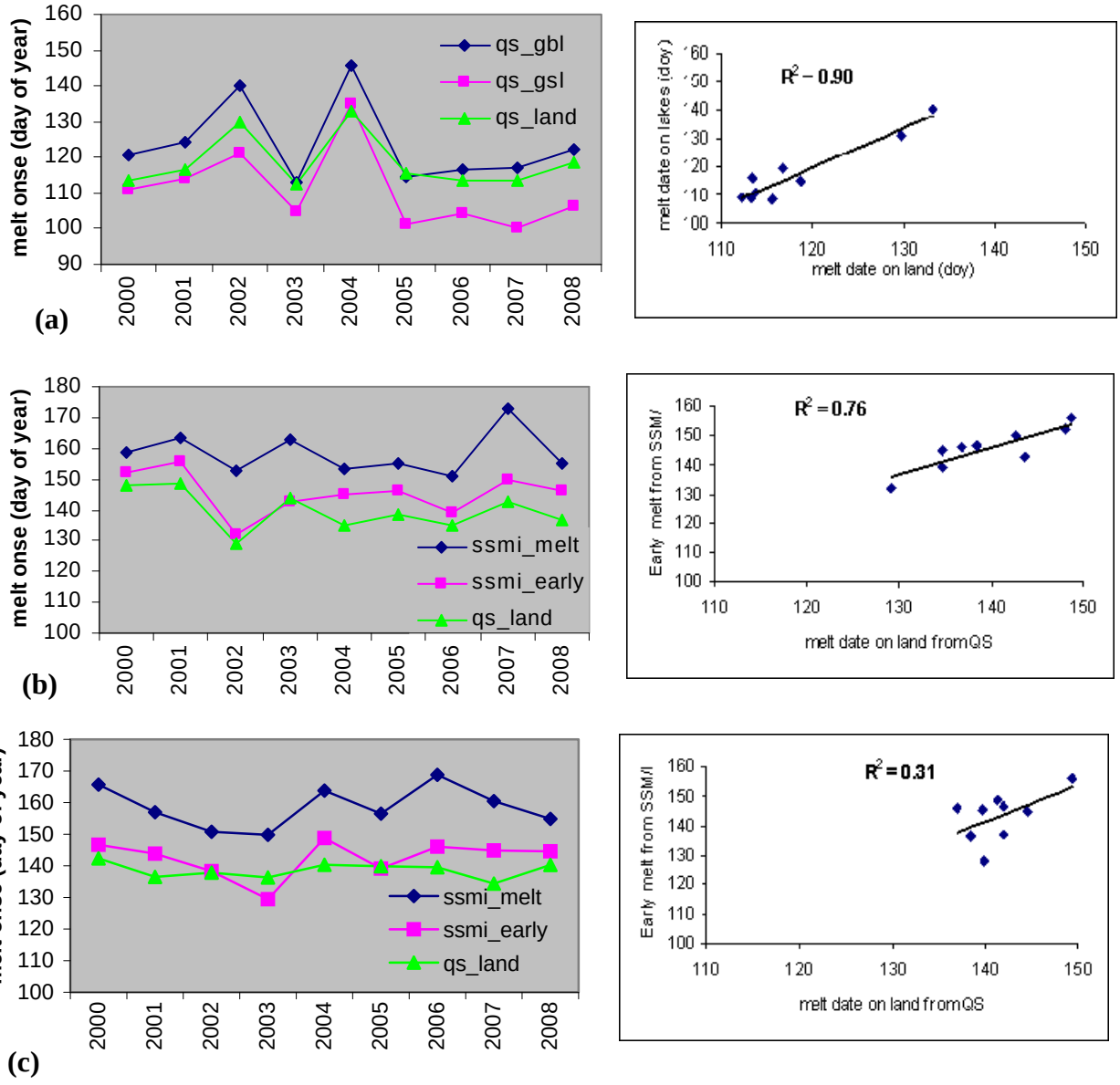

Figure 5. Line plots (left) and scatter plots (right) of annual mean melt onset from QS on land/lakes and from SSM/I on sea ice for selected sub-regions, (a) Great Bear Lake and Great Slave Lake and surrounding land; (b) Alaska coast; (c) east Siberia coast. Regions were shown in Fig 3a.

To verify the consistency of the integrated dataset across different cryosphere elements from different satellite data and different algorithms, annual mean melt onset dates in three sub-regions along the boundaries of land/lake ice and land/sea ice (polygons in Fig.3a) were examined. Line plots in Figure 5b and 5c show that the inter-annual variations in melt onset derived from QS on land and those derived from SSM/I on sea ice are generally coherent. Correlation analysis shows that melt on the Great Bear Lake and Great Slave Lake is closely correlated with melt on the surrounding land areas (Fig.5a, r^2=0.90). Along the Alaska coast, melt on sea ice from SSM/I is

highly correlated with melt on land from QS (Fig.5b, r^2=0.76). However, in east Siberia, melt on sea ice from SSM/I is not well correlated with melt on land from QS (Fig.5c, r^2=0.31). This is probably related to the less accurate sea ice melt onset detection in the marginal seas due to sea ice dynamics and ocean currents (Stroeve et al., 2006).

We also examined the annual mean melt onset on land and on sea ice in the QEI sea ice region (Fig.2). Although melt on sea ice from QS (yellow line in Fig.2) agrees better with SSM/I-derived early melt (pink line, r2=0.76), melt on land (green line) agrees better with SSM/I-derived melt onset (blue line, r2=0.81). One limitation in melt detection on terrestrial snow cover from QS data is that in regions with relatively thin snow cover (snow depth < 30 cm), such as in the QEI sea ice region (shown in Fig.2b), there may only be weak backscatter decreases during the melt period because a spatially continuous wet snow cover can be very transient. Thus melt may not always be detected in these thin snow cover regions. When melt was detected, it may bear a relatively high uncertainty compared to deeper snow cover regions (Wang et al., 2008). This is probably the main cause of the contrast seen in Figure 2.

SUMMARY

In this study, we generated an integrated melt onset dataset by combining estimates from optimized individual algorithms developed for the northern high latitude land surface, ice caps, large lakes, and sea ice. Evaluation of the dataset shows that the various algorithms perform consistently across most of the Arctic. Although we found the uncertainties are relatively high in regions where the sea ice is highly dynamic and where the snow cover is relatively thin, such regions are very limited and can be easily identified and excluded in further analyses. The integrated dataset presents the annual and inter-annual variability in melt timing across all elements of the cryosphere in the pan-Arctic.

Previous studies indicate that the satellite estimates of melt onset corresponded to a clear shift in the statistical distribution of daily mean air temperature from largely below freezing to above freezing (e.g. Wang et al., 2008). Therefore maps of melt onset provide a snap shot of the general climate conditions across the pan-Arctic in each spring. This is very useful information in the Arctic where the surface observation network is sparse. The integrated onset dataset also provides a unique tool to study the relationship among different components of the cryosphere and to investigate the atmospheric conditions associated with different melt onset patterns in the Arctic.

REFERENCES

Belchansky, GI. Douglas, DC. and Platonov, NG. 2004. Duration of the Arctic sea ice melt season: Regional and interannual variability, 1979-2001, *J Cim* **17**, 67-80.

Comiso, JC. Parkinson, CL. Gersten, R. and Stock, L. 2008. Accelerated decline in the Arctic sea ice cover. *Geophys Res Lett* **35**, L01703, doi:10.1029/2007GL031972.

Derksen, C. Brown, R. and Wang, L. 2009. Terrestrial Snow [in "State of the Climate in 2008"]. *Bull Amer Meteor Soc* **90**, S106-S107.

Drobot, SD. and Anderson, MR. 2001. An improved method for determining snowmelt onset dates over Arctic sea ice using scanning multichannel microwave radiometer and Special Sensor Microwave/Imager data, *J Geophys. Res* **106(24),** 033-24,049.

Haas, C. Pfaffling, A. Hendricks, S. Rabenstein, L. Etienne, J-L. and Rigor, I. 2008. Reduced ice thickness in Arctic Transpolar Drift favors rapid ice retreat, *Geophys Res Lett* **35**, L17501, doi:10.1029/2008GL034457.

Howell, SEL. Brown, LC. Kang, K.K. and Duguay, CR. 2009. Monitoring lake ice phenology variability on Great Bear Lake and Great Slave Lake, Northwest Territories, Canada, from SeaWinds/QuikSCAT: 2000-2006. *Remote Sensing of Environment* **113(4),** 816-834, doi:10.1016/j.rse.2008.12.007.

Howell, SEL. Tivy, A. Yackel, JJ. Scharien, RK. 2006. Application of a SeaWinds/QuikSCAT sea ice melt algorithm for assessing melt dynamics in the Canadian Arctic Archipelago. *J Geophys Res* **111**, C07025, doi:10.1029/2005JC003193.

Kay, J. E., L'Ecuyer, T., Gettelman, A., Stephens, G., and O'Dell, C. 2008. The contribution of cloud and radiation anomalies to the 2007 Arctic sea ice extent minimum, *Geophys. Res. Lett*., **35**, L08503, doi:10.1029/2008GL033451.

Perovich, D. K., Richter-Menge, J. A., Jones, K. F., and Light, B. 2008. Sunlight, water, and ice: Extreme Arctic sea ice melt during the summer of 2007, *Geophys. Res. Lett*., **35**, L11501, doi:10.1029/2008GL034007.

Perovich, D. K., Nghiem, S. V., Markus, T., and Schweiger, A. 2007. Seasonal evolution and interannual variability of the local solar energy absorbed by the Arctic sea ice–ocean system, *J. Geophys. Res*., **112**, C03005, doi:10.1029/2006JC003558.

Sharp, M., and Wang, L. 2009. A Five-Year Record of Summer Melt on Eurasian Arctic Ice Caps, *Journal of Climate*, **22**, 133-145.

Smith, D.M. 1998. Observation of perennial Arctic sea ice melt and freeze-up using passive microwave data, *J. Geophys. Res.,* **103**, 27,753-27,769.

Stroeve, J., Serreze, M., Drobot, S., Gearheard, S., Holland, M., Maslanik, J., Meier, W., and Scambos, T. 2008. Arctic sea ice extent plummets in 2007, *Eos Trans. AGU*, **89**(2), doi:10.1029/2008EO020001.

Stroeve, J., Markus, T., Meier, W., and Miller, J. 2006. Recent changes in the Arctic melt season, *Ann. Glaciol.,* **44**, 367-374.

Wang, L., Derksen, C., and Brown, R. 2008. Detection of snowmelt onset over the Pan-Arctic from QuikSCAT, 2000 – 2005. *Remote Sensing of Environment*, **112**, 3794 – 3805.

Wang, L., Sharp, M., Rivard, B., and Steffen, K. 2007. Melt season duration and ice layer formation on the Greenland ice sheet, 2000–2004, *J. Geophys. Res*., **112**, F04013, doi:10.1029/2007JF000760.